Long-term reliability of gate-oxide in Cascode GaN power devices under proton irradiation with different energies

Ru-Xue Bai[1], Hong-Xia Guo[2], Yang-Fan Li[1], Wu-Ying Ma[2], Ji-Fang Li[1], Feng-Qi Zhang[2], Xiao-Ping Ouyang[2], Xiang-Li Zhong[1]

Abstract In this paper, the effects of proton irradiation with different energies on the long-term reliability of gate-oxide in Cascode enhanced GaN power device is studied. The typical degradation of electrical properties was observed. In contrast, the gate current was increased by about two orders of magnitude after 25 MeV and 60 MeV proton irradiation, while the gate current was unchanged significantly after 100 MeV proton irradiation. By using time-dependent dielectric breakdown (TDDB) method confirms that the risk of gate current leakage is increased under proton irradiation. The breakdown time of gate dielectric becomes shorter after proton irradiation, which is not conducive to the long-term and stable application of GaN power devices. In addition, SRIM simulation results based on Monte Carlo indicated that the interaction cross section between low-energy protons and target nucleus is larger, which will cause more defects in the device, leading to the low-energy proton damage becomes more severe. Proton irradiation produces defects in the gate-oxide layer that shorten the breakdown time of the device gate-oxide layer, ultimately resulting the long-term reliability of the device was reduced.

This work was supported by the National Natural Science Foundationof China (Nos. 12275230 and 12027813)

✉ Hong-Xia Guo
guohxnint@126.com
✉ Xiang-Li Zhong
xlzhong@xtu.edu.cn

[1] The School of Materials Science and Engineering, Xiangtan University, Xiangtan 411105, China
[2] Northwest Institute of Nuclear Technology, Xi'an 710024, China

Keywords Proton irradiation · Cascode GaN power devices · Long-term reliability · TDDB · Monte Carlo simulation

1 Introduction

With the continuous development of high-power electric propulsion technology for space systems and satellite platforms, the devices with high-frequency, high-power, high-temperature, high-voltage and radiation-resistant have gradually become the development direction of high-efficiency power electronics systems [1-3]. As a typical representative of the third generation of wide band gap semiconductors, GaN materials have outstanding characteristics such as wide band gap (3.4 eV), high breakdown electric field (5×10^6 V/cm) and strong radiation resistance (10^{10} rad). This makes GaN-based power devices the most attractive candidates for space power systems [4-10]. Therefore, it is important to study the long-term reliability of GaN-based devices in space radiation environment.

Indeed, electronic devices working in aerospace will inevitably be damaged by energetic particles from complex radiation environment [11,12]. Among them, Protons are the most common particles in the space radiation environment, which has the characteristics of high energy and high fluence, and is a threat to aerospace electronic equipment [13,14]. Due to the high bond strength of N-Ga and N-Al in GaN HEMT devices, the resulting compounds such as GaN, AlN, and AlGaN exhibit high stability, which can generate a high displacement damage energy threshold (19 ~ 25 eV). Additionally, the two-dimensional electron gas (2DEG) in GaN is insensitive to defects, so GaN power devices have strong resistance to displacement damage. GaN has a wide bandgap and theoretically exhibits excellent resistance to ionizing radiation. However, in practice, GaN materials contain a high density of defects, and current GaN devices have high process requirements. These factors pose significant challenges to the radiation resistance characteristics of GaN power devices. Previous studies have shown that GaN-based devices are at risk of degradation or failure when exposed to radiation

environments [15-21].

Therefore, the effect of proton irradiation on GaN-based power devices cannot be ignored. A large number of proton irradiation experiments have been carried out for GaN-based power devices [22-27]. Yue et al [26]. performed a 3 MeV proton irradiation experiments on AlGaN/GaN HEMTs with a total fluence reached 5×10^{14} p/cm^2. The results show that the saturation current of the device is reduced by 14.6%, the threshold voltage (V_{th}) is shifted forward by 0.35 V and the inverse gate current is significantly reduced. The main degradation mechanism is thought to be an increase in the density of the negatively charged trap in the channel. Kim et al [27]. carried out proton irradiation experiments at 0.5 MeV, 5 MeV and 60 MeV on AlGaN/GaN HEMTs. The results show that the transfer properties decay the most after 0.5 MeV irradiation because the low proton energy produces a larger loss of non-ionizing energy. The gate leakage current of the fabricated HEMTs decreased by increasing the irradiation energy is due to the formation of interfacial oxide layer caused by proton radiation between gate and AlGaN layer. However, although these reports describe the degradation mechanisms of the electrical performance of GaN devices, they do not indicate the impact of these degradations on the lifespan of device. It is important to note that the most critical characteristic of aerospace components is long-term reliability. Therefore, further research is needed to achieve the long-term stable space application of GaN power devices.

In this work, the long-term reliability of the gate-oxide of Cascode GaN power devices is investigated for different energies of proton radiation. Using the time-dependent dielectric breakdown (TDDB) method, it was found that the time tolerance for gate oxide breakdown of the device after low-energy proton irradiation is the shortest. Furthermore, the SRIM simulation method was employed to elucidate the basic mechanism of the enhanced damage effect due to low-energy proton irradiation.

2 Sample and methods

2.1 Sample

The sample selected for this experiment are Common gate and Common source (Cascode) structure enhanced GaN power devices from Transphorm. The device is consisted of a high-voltage depletion GaN HEMT and a low-voltage enhanced Si MOSFET, and the device structure is shown in Fig. 1 (a). Since the drain source voltage of Si MOSFET provides a negative bias voltage to the gate-source voltage of GaN HEMT, the on-off of GaN HEMT can be controlled by controlling the on-off of Si MOSFET, thus achieving the normally closed characteristic. Fig. 1 (b) shows the device package diagram. We used FIB and SEM methods to analyze the layered structure of Cascode GaN power devices, and the results are shown in Fig. 1(c). The rated operating voltage of GaN power devices is 650 V, and the threshold voltage is 3.3 V ~ 4.8 V.

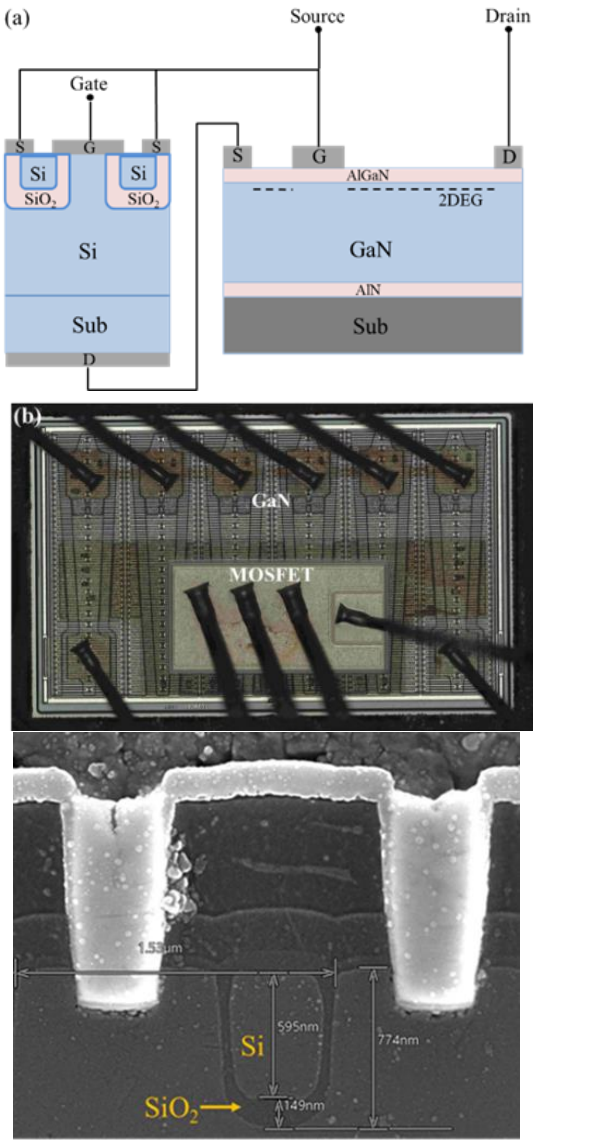

Fig. 1 a The structure diagram, **b** the package diagram, and **c** the SEM image of Cascode GaN power device.

2.2 Irradiation experiments

The proton experiment was carried out in Xi'an 200 MeV Proton Accelerator Facillity (XiPAF). Protons with energies of 25 MeV, 60 MeV and 100 MeV were used for experiments. The total fluence during the experiment was set to 2×10^{11} and 5×10^{11} p/cm^2, and the fluence rate was about 2×10^9 p/cm^2·s. The irradiation time is about 100 s~250 s. The bias voltage of 550 V, 600 V and 650 V were applied to the sample, respectively. The experimental temperature was room temperature. Irradiate two to three samples under each experimental condition to eliminate randomness.

2.3 Time-dependent dielectric breakdown methods (TDDB)

Since the 1990s, TDDB testing has been widely used for the quality assessment of gate oxide in power MOSFETs [28]. According to the method of applying the electric field to the device, TDDB lifetime prediction can be divided into constant voltage (current) and ramp voltage (current). In this article, we

use the constant voltage method, which can obtain the failure time of the device, evaluate the gate oxide quality of the device through Weibull distribution statistics, and further estimate the lifespan of the gate oxide layer. The constant voltage TDDB test is conducted at a voltage slightly lower than the gate breakdown voltage to determine the breakdown time and analyze the results. The slightly lower voltage itself is not sufficient to cause intrinsic breakdown. However, due to defects in the oxide layer during the application of electrical stress, after a certain period, charges accumulate near the defects or are captured by the defects, leading to breakdown. Time-dependent gate oxide breakdown is a major factor affecting device reliability. Generally speaking, breakdown occurs due to a high electric field and excessive current in the oxide layer, leading to charge accumulation.

2.4 Stopping and Range of Ions in Matter simulation method (SRIM)

SRIM uses the Monte Carlo method to track the motion of a large number of incident particles through computer simulation [29]. It is possible to calculate various physical processes of particle beams in different materials, including scattering, escape, energy deposition, transport, and the analysis of the radiation hardening characteristics of materials. The position of the particles, energy loss, and various parameters of secondary particles are all stored throughout the tracking process. The collision parameters are randomly selected to simulate the collision process, and calculate the process of incident ions colliding from the moment they enter the target until they lose energy and stop or exit the target. Finally, obtain the expected values of various required physical quantities and the corresponding statistical errors. Since the results of the calculations have statistical significance, only when the number of ions calculated is sufficiently large can the required calculation accuracy be achieved. SRIM provides two different interfaces: as shown in Figure 2 (a), the SRAM program interface allows users to input the state of the target material and the incident particles, and set the energy range of the incident particles. This interface is mainly used to calculate the penetration depth of particles with different energies in the target material. The other interface is the TRIM program interface, as shown in Figure 2 (b). Through this interface, users can calculate parameters related to energy loss of particle beams in target materials, the number of vacancies produced, and the slowing down of radiation damage to materials. In this article, the functionality of TRIM is mainly used.

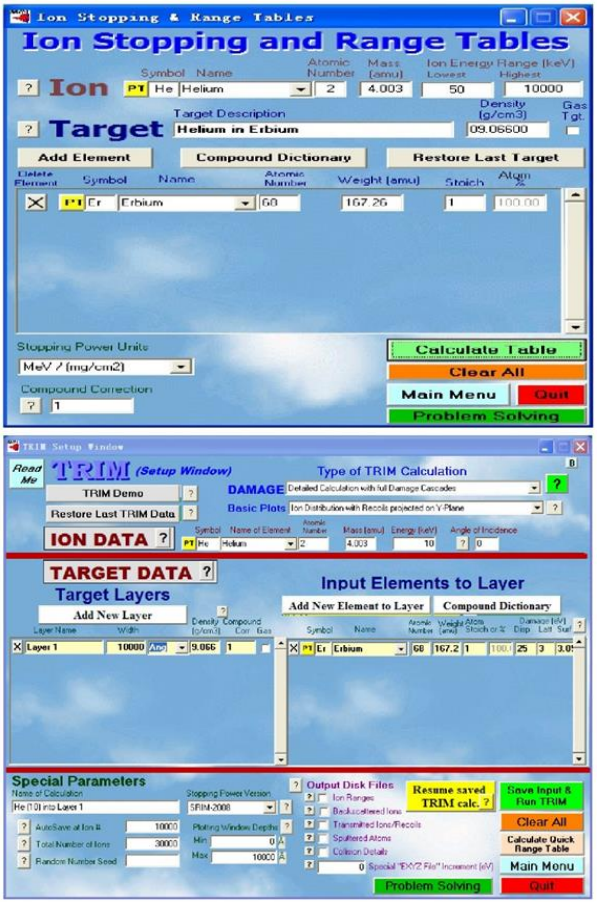

Fig. 2 a SRAM program interface and **b** TRIM program interface

3 Results and discussion

3.1 I-V characteristic results cc

The (I-V) characteristic curves of Cascode structure enhanced GaN power devices before and after proton irradiation are shown in Fig. 3. The device threshold voltage changes after proton irradiation with energies of 25 MeV, 60 MeV and 100 MeV are given in Fig. 3 (a). As can be seen in the figure, the threshold voltage of the devices shown negatively drifted after proton irradiation. The data are statistically presented in Table 1. The threshold voltage drift becomes more pronounced with the increase in proton fluence and bias voltage, which is consistent with previous experimental results [30-32]. The gate characteristics of the devices are represented by Fig. 3(b), from which it can be seen that the gate damage of the devices with 25 MeV and 60 MeV protons irradiation is more severe. After 25 MeV irradiation, the gate leakage current increases from 4.18×10^{-12} A to 4.42×10^{-10} A. After 60 MeV irradiation, the gate leakage current increased from 3.88×10^{-12} A to 3.81×10^{-10} A. The gate leakage current increases by two orders of magnitude. The gate characteristics of the devices are almost unchanged after 100 MeV proton irradiation. Fig. 3(c) shows the output characteristic curves of the device, which shows a slight increase in the drain leakage current after protons irradiation.

By comparing the changes in the electrical characteristics of the devices before and after proton irradiation, it is found that these degradations are mainly caused by gate damage. This is manifested as the negative drift of threshold voltage and the increase of gate leakage current. The threshold voltage negative drift indicates that the switching capability of the gate is degraded. The gate characteristics of the Cascode GaN power device are mainly controlled by the Si MOSFETs, as can be seen from the presentation in Fig. 1(a). For gate oxide transistors, the threshold voltage drift is due to a combination of oxide trap charge and interface trap charge [33]:

Fig. 5 I_D-V_D curve diagram of Cascode GaN power device (a) 25 MeV, (b) 60 MeV, (c) 100 MeV.

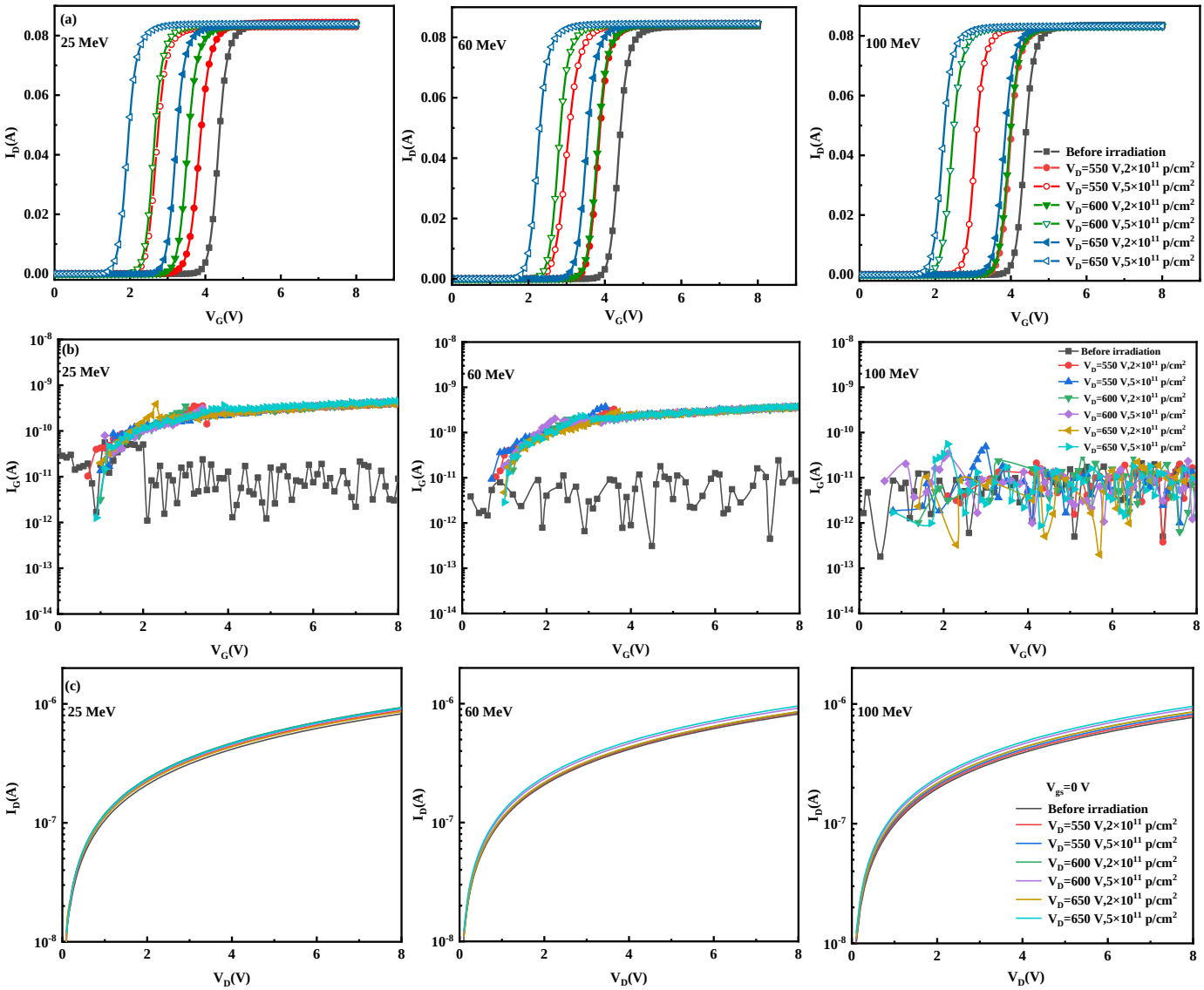

Fig. 3 Electrical characterization diagram of Cascode GaN power device **a** I_D-V_G, **b** I_G-V_G, and **c** I_D-V_D.

$$\Delta V_{th} = \Delta V_{ot} + \Delta V_{it}, \tag{1}$$

$$\Delta V_{ot,it} = \frac{-1}{C_{ox} t_{ox}} \int_0^{t_{ox}} \rho_{ot,it}(x) x dx. \tag{2}$$

where ΔV_{ot} is the oxide trap charge, ΔV_{it} is the interface trap charge, C_{OX} is the capacitance per unit area of the gate oxide layer, t_{ox} is the oxide layer thickness, and $\rho_{ot,it}(x)$ is the charge distribution of the radiation-induced oxide trap charge or interface trap charge. At high dose rates and short periods of time, the neutralization of the oxide trap charge is small, resulting in a high oxide trap charge density. In contrast, interfacial trap charges do not have enough time to accumulate and usually have small densities [33]. In other words, the oxide trap charge generated by proton irradiation plays a major role in the threshold voltage drift. The increase of gate leakage current indicates the deterioration of insulation characteristics of gate. The degradation of the insulating properties of the gate oxide is usually caused by defects or conductive channels generated by localized hot carrier stresses in the drain [34]. From the above analysis, it can be concluded that the defects generated in the oxide layer are the main reason for the degradation of the device gate characteristics due to proton irradiation.

3.2 TDDB test results and discussion

In order to reveal the effect of proton irradiation introducing defects in the gate oxide layer on the long-term reliability of the gate oxide layer of Cascode GaN power device, we will compare the breakdown time of gate dielectric before and after irradiation using the TDDB experimental method. TDDB experiment adopts the constant voltage stress (CVS) method. First, the time-zero dielectric breakdown (TZDB) method is used to determine the accelerated stress test range. It is specified that the breakdown occurs when the gate current reaches 0.1 A.

Table 1 The threshold voltage of Cascode GaN power device under various proton energies and bias voltages.

Energy	Bias	$V_{th}(V)_{non\text{-}radiation}$	$V_{th}(V)_{radiation}$	
			2×10^{11} p/cm^2	5×10^{11} p/cm^2
	550 V		2.8	1.7
25 MeV	600 V	3.4	2.6	1.7
	650 V		2.3	1
	550 V		2.8	1.9
60 MeV	600 V	3.4	2.8	1.8
	650 V		2.5	1.3
	550 V		2.9	2.1
100 MeV	600 V	3.4	2.8	1.9
	650 V		2.6	1.6

As shown in Fig. 4(a), when the gate voltage reaches about 47 V, the device will be broken down instantly. In order to complete the experiment more accurately and quickly, the bias voltage V_{GS}=45 V is selected in the TDDB test. Fig. 4(b) shows the curve of the gate leakage current of the devices before and after proton irradiation as a function of time under constant stress at the gate. As can be seen from the figure, the device gate leakage current continues to decrease before breakdown. This is the gate breakdown characteristic of silicon-based devices, which further indicates that the gate damage caused by proton irradiation is dominated by the damage of cascading Si-based transistors. The decrease in current indicates that the net negative charge in the device is captured [35]. The breakdown time of the unirradiated devices is about 28225 s. After 100 MeV proton irradiation of the device, the breakdown time is almost constant, about 27985 s. The breakdown time of the device after 60 MeV proton irradiation is about 26892 s, which is shortened by about 4.72%. The breakdown time of the device after 25 MeV proton irradiation is about 22535 s, which is shortened by about 20.16%.

The TDDB failure models widely used at present include E model and 1/E model [36,37]. The E model also known as the thermochemical model, is suitable for devices with thicker gate oxide layers. The 1/E model is more suitable for devices with gate oxide layer thickness <5 nm. As shown in Fig. 1(c), the thickness of the gate oxide layer of the experimental sample is about 149 nm, so the E model should be used for failure analysis. The basic idea of the E model is that as the defects in the oxide layer increase, when the defects in the oxide layer are connected into a leakage path, the oxide layer will break down. Fig. 5 shows a schematic diagram of the leakage paths in the oxide layer before and after proton irradiation. When a high voltage is applied between the upper and lower interfaces of the oxide layer, the defects in the oxide layer will form electron traps, randomly distributed within the oxide layer. Each electron trap has the ability to capture electrons under influence of the electric field in the oxide layer. After proton irradiation, the number of defects in the oxide layer increases, and the regions where electron traps capture electrons may overlap, forming a current path from the upper interface of the oxide layer to the lower interface, as shown in Fig. 5(b). Therefore, proton irradiation leads to a reduction in the gate-oxide layer breakdown time of the device.

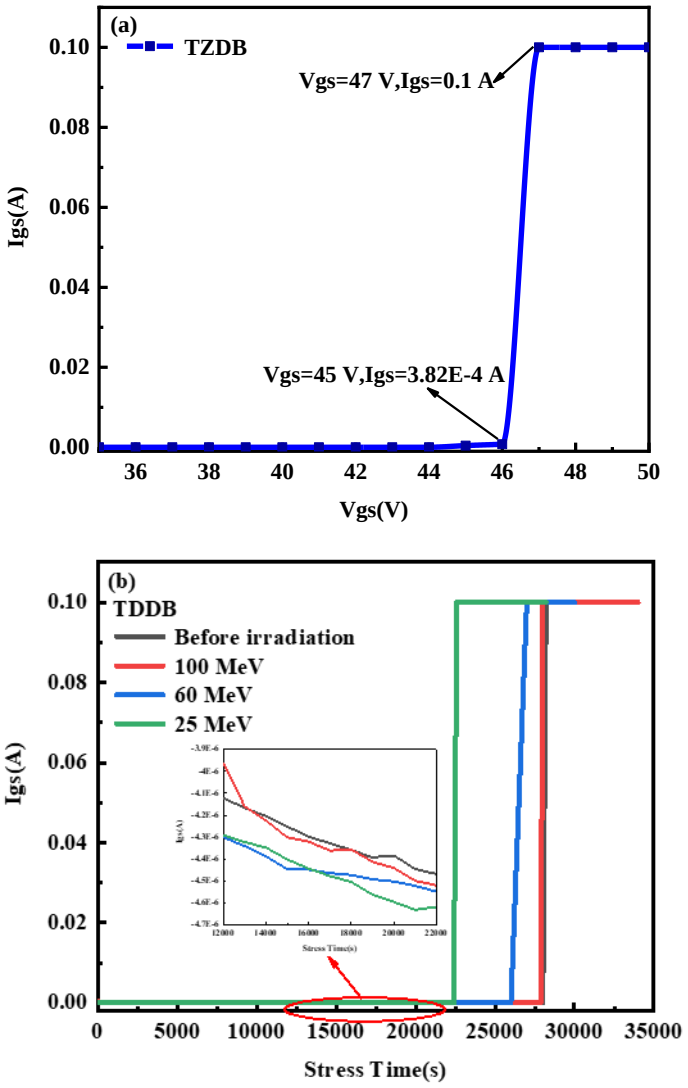

Fig. 4 a Time-zero dielectric breakdown test curve, **b** time-dependent dielectric breakdown test curve.

It is also common to utilize the gate oxide layer cumulative charge to assess the magnitude of the device breakdown time, and thus the gate oxygen layer lifetime. The cumulative charge is shown by eq. 3 [34]:

$$Q_{BD} = \int_0^{t_{BD}} Jdt \tag{3}$$

Where t_{BD} is the gate-oxide breakdown time; J is the gate leakage current. According to the calculation, Q_{BD} is 0.197 C before proton irradiation, Q_{BD} is 0.212 C after 100 MeV proton irradiation, Q_{BD} is 0.275 C after 60 MeV proton irradiation, and Q_{BD} is 0.299 C after 25 MeV proton irradiation, which increases by 40% compared with before irradiation. The accumulated charge of the gate oxide layer increases after irradiation and the lifetime of the gate oxide layer decreases. This charge-to-breakdown value has been used for several years as the most important reliability figure- of-merit for oxides.

3.2 SRIM simulation results and discussion

Through the analysis of proton irradiation experiment and TDDB experiment results, it is found that the influence of 100

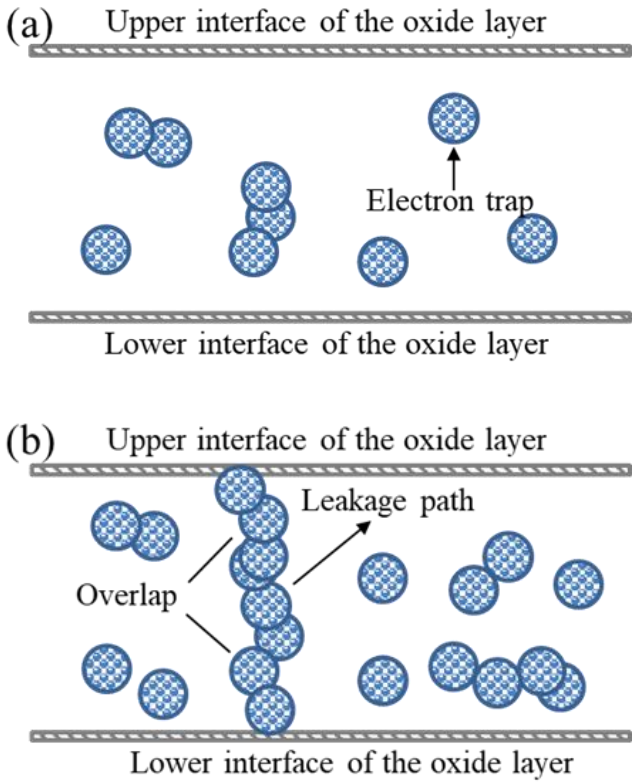

Fig. 5 Schematic diagram of the leakage paths in the oxide layer **a** before and **b** after proton irradiation.

MeV proton irradiation on the device is smaller than 25 MeV and 60 MeV, and the phenomenon of low energy damage is more serious. This is due to the fact that protons travel essentially in a straight line through the material. The higher proton energy, the smaller interaction cross section between the proton and the target nucleus, and the smaller average energy transferred to the target nucleus [38,39]. With the increase of proton energy, the radiation damage region gradually moves deeper into the device, away from the sensitive gate oxide layer region. We simulated the interaction cross sections between proton at different energies and target using SRIM software, as shown in Fig. 6. The simulation results confirm the above statement that the irradiation damage region gradually moves away from the gate oxide layer as the proton energy increases (marked by the red arrow). The interaction radii of protons at 25 MeV, 60 MeV, and 100 MeV are 6×10^{-8}, 2.8×10^{-8} and 2×10^{-8} Ang/Ion, respectively. In comparison, the cross-sectional radius produced by 25 MeV proton irradiation (circled in red dashed lines) is the largest. We also simulated the number of vacancies generated by protons of different energies in Si MOSFET transistors, as shown in Fig. 6(d). Among them, the 25 MeV protons produce the most vacancy defects in the device's sensitive layer. These two factors eventually lead to enhanced damage of low-energy proton irradiation. The simulation results are consistent with the experimental analysis results. The simulation results and the experimental analysis results have mutually verified each other.

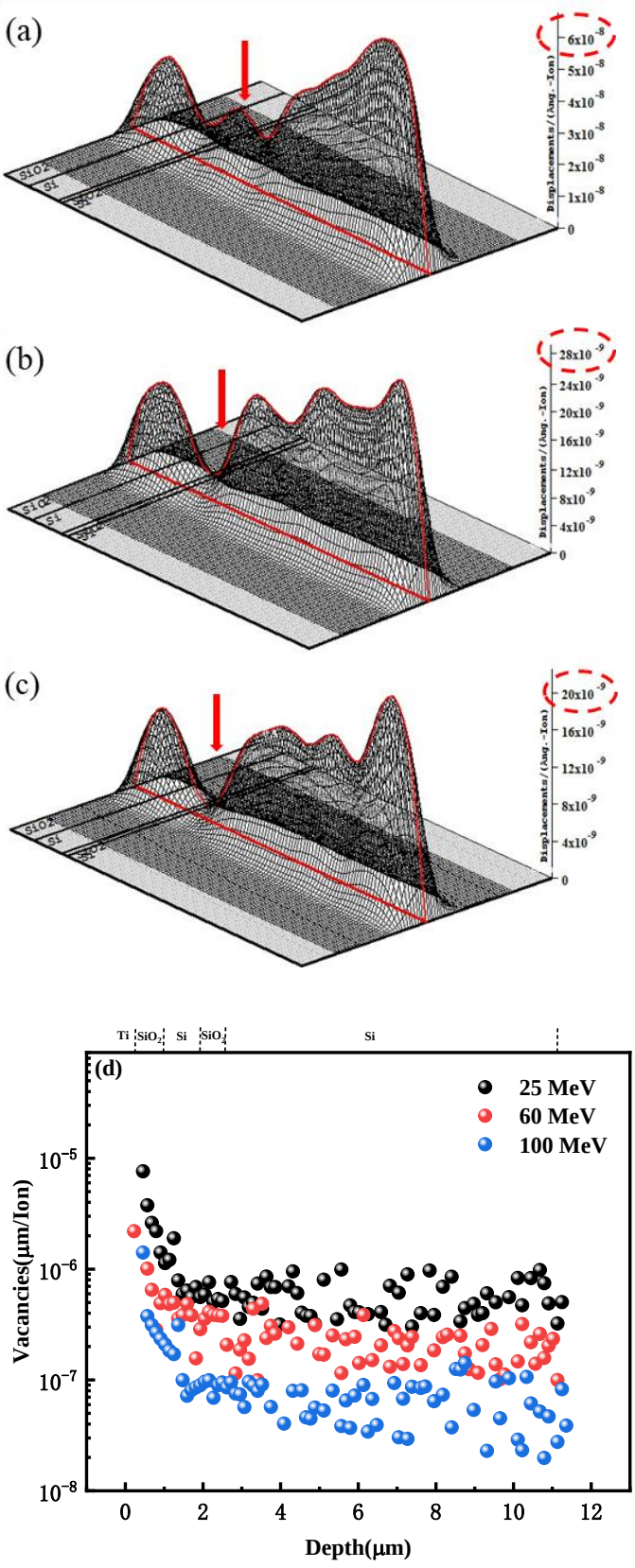

Fig. 6 Trajectory diagram of proton incident Cascode GaN power device **a** 25 MeV **b** 60 MeV **c** 100 MeV and **d** the vacancy.

4 Conclusion

In summary, the impact of proton irradiation at different energies on the long-term reliability of the gate oxide in the Cascode GaN power devices has been investigated. Through the analysis of experimental results combined with the device electrical characteristics formula, the oxide trap charges introduced by proton irradiation in the oxide layer are the main factors leading to the deterioration of the device's gate performance. The degradation of gate performance indicates that gate switching capability and gate insulation characteristics are damaged, which is detrimental to the long-term reliable application of the device. To this end, we used the TDDB experimental method to test the gate tolerance of the device before and after proton irradiation. We applied a constant gate bias voltage of V_{GS}=45 V to both the unirradiated and irradiated devices. The experimental results show that the gate dielectric breakdown time of the irradiated device becomes shorter and the lifetime of the gate oxide layer of the device decreases. This is because proton irradiation introduces defects in the device's oxide layer, which form electron traps that capture electrons under the influence of an electric field. The accumulation of a large number of electron traps will form one or more channels from the upper interface of the oxide layer to the lower interface, which serve as leakage paths. When the traps capture enough electrons, the device gate will undergo breakdown. Furthermore, it has been found that 25 MeV and 60 MeV protons cause more damage to the device than 100 MeV protons. We used the SRIM method to simulate the interaction between protons of different energies and the device, which well explained this phenomenon. The simulation results indicate that 25 MeV proton irradiation introduces more vacancy defects into the device. The radiation damage area of low-energy protons is closer to the device's sensitive area and has a larger effective range. The results of this paper can provide theoretical support for further improving the long-term reliability of gate oxide in Cascode GaN power devices.

Author contributions All authors contributed to the study conception and design. Material preparation, data collection and analysis were performed by Ru-Xue Bai, Hong-Xia Guo, Yang-Fang Li, Wu-Ying Ma and Ji-Fang Li. The first draft of the manuscript was written by Ru-Xue Bai and all authors commented on previous versions of the manuscript. All authors read and approved the final manuscript.

Data availability The data that support the findings of this study are openly available in Science Data Bank.

References

1. B. Mounika, J. Ajayan, S. Bhattacharya, et al., Recent developments in materials, architectures and processing of AlGaN/GaN HEMTs for future RF and power electronic applications: A critical review. Micro and Nanostructures. **168** , 207317 (2022). https://doi.org/10.1016/j.sse.2022.108571
2. Y. Yuan, S. Q. Zhou, X. Q. Wang, Modulating properties by light ion irradiation: From novel functional materials to semiconductor power devices. Journal of Semiconductors. **43**, 063101 (2022). https://doi.org/10.1088/1674-4926/43/6/063101
3. Y. Tang, L. Wang, X. W. Cai, et al., Investigation on performance degradation mechanism of GaN p–i–n diode under proton irradiation. Appl. Phys. Lett **122**, 022101 (2023). https://doi.org/10.1063/5.0130017
4. N. R. Glavin, K. D. Chabak, E. R. Heller, et al., Flexible gallium nitride for high-performance, strainable radio-frequency devices. Adv. Mater **29**, 1701838 (2017). https://doi.org/10.1002/adma.201701838
5. X. Li, P. E. Wang, X. Zhao, et al., Defect and impurity-center activation and passivation in irradiated AlGaN/GaN HEMTs. IEEE Trans. Nucl. Sci. **71**, 80-87 (2024). https://doi.org/10.1109/TNS.2023.3336836
6. W. J. Yan, Y. Y. Xue, W. J. Zhou, et al., Au ion irradiation induces ultralow thermal conductivity in GaN. Appl. Phys. Lett **125**, 032202 (2024). https://doi.org/10.1063/5.0220863
7. D. M. Fleetwood. E. X. Zhang, R. D. Schrimpf, et al., Radiation effects in AlGaN/GaN HEMTs. IEEE Trans. Nucl. Sci. **69**, 1105-1119 (2022). https://doi.org/10.1109/TNS.2022.3147143
8. S. J. Pearton, R. Deist, F. Ren, et al., Review of radiation damage in GaN-based materials and devices. J. Vac. Sci. Technol. A. **31**, 050801 (2013). https://doi.org/10.1116/1.4799504
9. T.P. Chow, R. Tyagi, Wide bandgap compound semiconductors for superior high-voltage unipolar power devices. IEEE Trans. Electron Dev. Sci. **41**, 1481–1483 (1994). https:// doi. org/ 10. 1109/ISPSD.1993.297113
10. W. Saito, Y. Takada, M. Kuraguchi et al., High breakdown voltage AlGaN/GaN power-HEMT design and high current density switching behavior. IEEE Trans. Electron Dev. Sci. 50, 2528-2531 (2003). https://doi.org/10.1109/TED.2003.819248
11. J M. Osheroff, J. M. Lauenstein, R. L. Ladbury, LET and range characteristics of proton recoil ions in gallium nitride (GaN). IEEE Trans. Nucl. Sci. **68**, 597-602 (2021). https://doi.org/10.1109/TNS.2021.3050980
12. F. Mirkhosravi, A. Rashidi, A. T. Elshafiey, et al., Effects of fast and thermal neutron irradiation on Ga-polar and N-polar GaN diodes. J. Appl. Phys. **133**, 015704 (2023). https://doi.org/10.1063/5.0119294
13. R. Ecoffet, Overview of in-orbit radiation induced spacecraft anomalies. IEEE Trans. Nucl. Sci. **60**, 1791-1815 (2013). https://doi.org/ 10.1109/TNS.2013.2262002
14. H. Zhang, H. X. Guo, F. Q. Zhang, et al., Study on proton-induced single event effect of SiC diode and MOSFET. Microelectron. Reliab. **124**, 114329(2021). https://doi.org/10.1016/j.microrel.2021.114329
15. L. Lv, J. G. Ma, Y. R. Cao, et al., Study of proton irradiation effects on AlGaN/GaN high electron mobility transistors. Microelectron. Reliab. **51**, 2168-2172 (2011). https://doi.org/10.1016/j.microrel.2011.04.022

16. S.J. Pearton, F. Ren, E. Patrick et al., Review-Ionizing radiation damage effects on GaN devices. ECS J. Solid State Sci. Technol **5**, Q35–Q60 (2016). https://doi.org/10.1149/2.02516 02jss
17. A.Y. Polyakov, S.J. Pearton, P. Frenzer et al., Radiation effects in GaN materials and devices. J. Mater. Chem. C. Sci. **5**, 877-887 (2013). https://doi.org/10.1039/C2TC00039C
18. L.Q. Zhang, C.H. Zhang, C.L. Xu et al., Damage produced on GaN surface by highly charged Krq+ irradiation. Nucl. Sci. Tech. **28**, 176 (2017). https://doi.org/10.1007/s41365-017-0326-4
19. C. H. Sun, C. Peng, Z. G. Zhang, et al., Mechanism of reverse gate leakage current reduction in AlGaN/GaN high-electron-mobility-transistor after 3-MeV proton irradiation. Appl. Phys. Lett. **121**, 072109 (2022). https://doi.org/10.1063/5.0102366
20. G.P. Liu, X. Wang, M.N. Li et al., Effects of high-energy proton irradiation on separate absorption and multiplication GaN avalanche photodiode. Nucl. Sci. Tech. **29**, 139 (2018). https:// doi.org/10.1007/s41365-018-0480-3
21. P. P. Hu, L. J. Xu, S. X. Zhang, et al., Failure mechanisms of AlGaN/GaN HEMTs irradiated by high-energy heavy ions with and without bias. Nucl. Sci. Tech. **36**, 13 (2025). https://doi.org/10.1007/s41365-024-01567-2
22. Z. Zhang, A. R. Arehart, E. Cinkilic, et al., Impact of proton irradiation on deep level states in n-GaN. Appl. Phys. Lett. **103**, 042102 (2013). https://doi.org/10.1063/1.4816423
23. X. Wan, O. K. Baker, M. W. McCurdy, et al., Low energy proton irradiation effects on commercial enhancement mode GaN HEMTs. IEEE Trans. Nucl. Sci. **64**, 253-257 (2017). https://doi.org/10.1109/TNS.2016.2621065
24. A. Stockman, A. Tajalli, M. Meneghini, et al., The effect of proton irradiation in suppressing current collapse in AlGaN/GaN high-electron-mobility transistors. IEEE Trans. Electron Dev. Sci. 66, 372-377 (2019). https://doi.org/10.1109/TED.2018.2881325
25. T. Zhu, X. F. Zheng, T. X. Yin, et al., A thorough study on the electrical performance change and trap evolution of AlGaN/GaN MIS-HEMTs under proton irradiation. Appl. Phys. Lett. **122**, 183502 (2023). https://doi.org/10.1063/5.0146638
26. S. Z. Yue, Z. F. Lei, C. Peng, et al., High-fluence proton-induced degradation on AlGaN/GaN high-electron-mobility transistors. IEEE Trans. Nucl. Sci. **67**, 1339-1344 (2020). https://doi.org/10.1109/TNS.2020.2974916
27. D. S. Kim, J. H. Lee, J. G. Kim, et al., Anomalous DC characteristics of AlGaN/GaN HEMTs depending on proton irradiation energies. ECS J. Solid State Sci. Technol. **9**, 065005 (2020). https://doi.org/10.1149/2162-8777/aba32e
28. M. M. Mathur, J. A. Cooper, Time-dependent-dielectric-breakdown measurements of thermal oxides on n-type 6H-SiC. IEEE Trans. Electron Dev. Sci. 46, 520-524 (1999). https://doi.org/10.1109/16.748871
29. J. F. Ziegler, M. D. Ziegler, J. P. Biersack, SRIM – The stopping and range of ions in matter. Nucl. Instrum. Methods, B. 268, 1818-1823 (2010). https://doi.org/10.1016/j.nimb.2010.02.091
30. Y. X. Lu, R. X. Cao, H. X. Li, et al., Degradation of electrical performance and radiation damage mechanism of cascode GaN HEMT with 80 MeV proton. Phys. Scr. **99**, 035920 (2024). https://doi.org/10.1088/1402-4896/ad22c5
31. X. W. Hu, A. P. Karmarkar, B. Jun, et al., Proton-irradiation effects on AlGaN/AlN/GaN high electron mobility transistors. IEEE Trans. Nucl. Sci. **50**, 1791-1796 (2003). https://doi.org/10.1109/TNS.2003.820792
32. R. D. Harris, L. Scheick, J. P. Hoffman, et al., Radiation Characterization of Commercial GaN Devices. IEEE Radiation Effects Data Workshop, Las Vegas, NV, USA, 1-5 (2011). https://doi.org/10.1109/REDW.2010.6062526
33. J. R. Schwank, M. R. Shaneyfelt, D. M. Fleetwood, et al., Radiation effects in MOS oxides. IEEE Trans. Nucl. Sci. **55**, 1833-1853 (2008). https://doi.org/10.1109/TNS.2008.2001040
34. G. Groeseneken, R. Degraeve, T. Nigam, et al., Hot carrier degradation and time-dependent dielectric breakdown in oxides. Microelectronic Engineering **49**, 27-40 (1999). https://doi.org/10.1016/S0167-9317(99)00427-X
35. P. Hazdra, P. Smrkovsky, J. Vobecky et al., Radiation resistance of high-voltage silicon and 4H-SiC power pin diodes. IEEE Trans. Electron Dev. Sci. **68**, 202-207 (2020). https://doi.org/10.1109/TED.2020.3038713
36. J. W. McPherson, H. C. Mogul, Underlying physics of the thermochemical E model in describing low-field time-dependent dielectric breakdown in SiO_2 thin films. J. Appl. Phys. **84**, 1513-1523 (1998). https://doi.org/10.1063/1.368217
37. J. W. McPherson, V. K. Reddy, H. C. Mogul, Field-enhanced Si–Si bond-breakage mechanism for time-dependent dielectric breakdown in thin-film SiO_2 dielectrics. J. Appl. Phys. **71**, 1101-1103(1997). https://doi.org/10.1063/1.119739
38. I. Jun, M. A. Xapsos, S. R. Messenger, et al., Proton nonionizing energy loss (NIEL) for device applications. IEEE Trans. Nucl. Sci. **50**, 1924-1928 (2003). https://doi.org/10.1109/TNS.2003.820760
39. S. R. Messenger, E. A. Burke. G. P. Summers, et al., Nonionizing energy loss (NIEL) for heavy ions. IEEE Trans. Nucl. Sci. **46**, 1595-1602 (1999). https://doi.org/10.1109/23.819126